Adsorption and Desorption of DNA on Graphene Oxide Studied by Fluorescently Labeled Oligonucleotides

Marissa Wu, Ravindra Kempaiah, Po-Jung Jimmy Huang, Vivek Maheshwari, and Juewen Liu**

Department of Chemistry, Waterloo Institute for Nanotechnology, University of Waterloo, 200 University Avenue West, Waterloo, Ontario, N2L 3G1, Canada

liujw@uwaterloo.ca; vmaheshw@uwaterloo.ca

Received: September 22, 2010
Revised: January 14, 2011
Published: February 08, 2011

ABSTRACT

Being the newest member of the carbon materials family, graphene possesses many unique physical properties resulting is a wide range of applications. Recently, it was discovered that graphene oxide can effectively adsorb DNA and at the same time, it can completely quench adsorbed fluorophores. These properties make it possible to prepare DNA-based optical sensors using graphene oxide. While practical analytical applications are being demonstrated, the fundamental understanding of binding between graphene oxide and DNA in solution received relatively less attention. In this work, we report that the adsorption of 12, 18, 24, and 36-mer single-stranded DNA on graphene oxide is affected by several factors. For example, shorter DNAs are adsorbed faster and bind more tightly to the surface of graphene. The

adsorption is favored by a lower pH and a higher ionic strength. The presence of organic solvents such as ethanol can either increase or decrease adsorption depending on the ionic strength of the solution. By adding the complementary DNA, close to 100% desorption of the absorbed DNA on graphene can be achieved. On the other hand, if temperature is increased, only a small percentage of DNA is desorbed. Further, the adsorbed DNA can also be exchanged by free DNA in solution. These findings are important for further understanding the interactions between DNA and graphene and for the optimization of DNA and graphene based devices and sensors.

Introduction

Graphene is the newest member of the carbon materials family.[1-4] Since its discovery, graphene has attracted wide research interests because of its unique physical properties such as superior electric conductivity and excellent mechanical strength.[2] It has been used for making flexible screens and organic light emitting diodes.[5,6] In addition graphene has also been found useful in designing chemical and biological sensors.[7] Being a single atomic layer of graphite, the conduction of electrons and holes in graphene is highly sensitive to surface conditions.[8,9] At the same time, graphene has an extremely large surface-to-volume ratio to interface with biomolecules. In combination with the high mobility of charge carriers and their high density in the graphene sheets,[1,10,11] changes in surface conditions due to binding of proteins and hybridization of DNA can be detected electrically.[12-14]

Recently, graphene (and graphene oxide) has also been used in making DNA-based optical sensors for the detection of nucleic acids,[15-20] proteins,[21,22] virus,[23] metal ions,[24] and small molecules[25-27] and for drug delivery.[28-30] Graphene is a hydrophobic material. To improve its solubility in water, graphene is oxidized to graphene oxide (GO) by generating surface carboxylic acid and hydroxyl groups. Most GObased DNA optical sensors use a reaction scheme depicted in Figure 1A (reaction 1). Under this scheme, on mixing a fluorophore-labeled single-stranded (ss) probe DNA with GO, the DNA is adsorbed

on the GO surface and its fluorescence is quenched. Upon addition of the target DNA, the probe DNA is desorbed from the GO surface forming double-stranded (ds) DNA in solution, restoring the fluorescence signal.[15] Such applications are possible because of two unique properties of GO. First, GO is capable of binding to ss-DNA with a high affinity; while the affinity for ds-DNA or well-folded ss-DNA is much lower. Second, GO is a universal fluorescence quencher;[16] many organic dyes and quantum dots can be effectively quenched by GO.[17] With both properties, sensitive fluorescent sensors with a high signal-to-noise ratio can be constructed using GO and DNA.

While practical analytical applications of GO have been successfully demonstrated, this study provides complementary information to understand the binding interactions between GO and DNA.[31]

Previous work has focused on characterization of the adsorption of single nucleotides or nucleosides by atomic force microscopy (AFM),[32] isothermal titration calorimetry,[33] and theoretical calculations.[34-36] It was concluded that non-electrostatic interactions dominate the binding,[32] and the purine bases bind more strongly than the pyrimidines.[33,35,36] The adsorption of DNA on carbon nanotubes has also been studied.[37-43] GO and nanotubes, however, are fundamentally different and the adsorption/desorption of oligonucleotides on GO have not been systematically tested as a function of solution conditions. We believe such studies can serve as a basis for further design and optimization of GO and DNA-based biosensors. Herein, we report the effect of DNA length, pH, salt, and solvent on DNA binding to GO. Further desorption of DNA by complementary DNA (c-DNA), temperature and the exchange of the adsorbed DNA are also studied.

Materials and Methods

Chemicals. All DNA samples were purchased from Integrated DNA Technologies (Coralville, IA). The DNA sequences are: 12-mer, CAC TGA CCT GGG; 18-mer, CTT GAG AAA GGG CTG CCA; 24mer, ACG CAT CTG TGA AGA GAA CCT GGG; and 36-mer, TAC CTG GGG GAG TAT TGC GGA

GGA AGG TTC CAG GTA. All the sequences are listed from the 5′ to 3′-end. Each DNA carries a FAM (6-carboxyfluorescein) modification on the 5′-end. Sodium chloride, magnesium chloride, sodium acetate, 4-Morpholineethanesulfonate (MES), 4-(2-hydroxyethyl)piperazine-1-ethanesulfonate (HEPES), and Tris(hydroxymethyl)aminomethane (Tris) were purchased from Mandel Scientific (Guelph, Ontario, Canada). Sulfuric acid, potassium persulfate, phosphorous pentoxide, hydrogen peroxide, potassium permanganate were purchased from Sigma-Aldrich. Acetic acid and hydrochloric acid were purchased from VWR. Graphite flakes were purchased from Fisher.

Synthesis of GO. GO was synthesized using the modified Hummers method.[44,45] Briefly, 3 g of graphite flakes (~325 mesh size) were dissolved in 10 mL of sulfuric acid (H_2SO_4). Potassium persulfate ($K_2S_2O_8$) and phosphorous pentoxide (P_2O_5) were added to the solution as oxidizing agents and stirred at 90 °C until the flakes were dissolved. The solution was stirred at 80 °C for 4 hrs and subsequently diluted with 500 mL water. The diluted solution was stirred overnight, washed and filtered to get a dry powder. This pre-oxidized GO powder was subjected to further oxidation with 125 mL of H_2SO_4 and 15 g of $KMnO_4$ in an ice bath and stirred for 2 hrs. 130 ml of water was added to the solution causing the temperature to rise to 95 °C. After 15 minutes, 15 mL of H_2O_2 was added. Finally the solution was diluted with 400 mL water and the resultant yellow-brown suspension was stirred overnight. This GO solution was filtered and washed until it reached a neutral pH and also purified by dialysis to remove excess ions. Finally, the GO solution was suspended at a concentration of 200 μg/mL.

Adsorption Efficiency. The DNA adsorption experiments were carried out based on the assumption that upon adsorption, the FAM fluorescence was completely quenched. In a typical experiment, a solution of 20 μL was prepared to contain 1 μM of FAM-labeled DNA, 170 μg/mL GO, and varying concentrations of buffer and salt. Another sample without GO was also prepared for comparison. The DNA was allowed to mix with GO for ~5 min at room temperature and the fluorescence was read by a real-time PCR thermocycler (Bio-Rad, CFX96) in the FAM channel. The temperature was set at 25 °C. For NaCl-dependent adsorption, the buffer contained 25 mM HEPES, pH 7.6. For $MgCl_2$-dependent adsorption, 25

mM Tris-HCl, pH 8.0 was used. The adsorption efficiency was calculated by the equation (F_{noGO}-F_{GO})/F_{noGo}, where F_{noGO} and F_{GO} are the fluorescence intensity in the absence and presence of GO, respectively.

Effect of pH. To study the effect of pH, the following buffer solutions were prepared: acetate buffer (pH 4.0 and 5.0), MES (pH 6.0), Tris-HCl (pH 7.0 and 8.0). Each sample (40 μL) contained a final buffer concentration of 50 mM, 10 mM NaCl, 170 μg/mL GO and 1 μM of the 36-mer DNA. After 1 hr incubation at room temperature for binding, the solutions were centrifuged at 15000 rpm for 20 min. 20 μL of the supernatant solution was transferred into another tube containing 200 μL of buffer (100 mM Tris HCl, pH 8.3) and the samples were measured by a fluorescence plate reader (Molecular Devices, SpectraMax 5) by exciting at 485 nm. Another sample at pH 8.0 with the same DNA concentration but without GO was also prepared for comparison.

Kinetics of Binding. The kinetics of binding was studied by adding 20 μL of GO solution to 80 μL of DNA solution. Several different DNA, GO, and salt concentrations were tested. The fluorescence before GO addition was also measured to be the value for time zero. The fluorescence change was monitored by the plate reader at room temperature (25 °C).

Effect of Ethanol. Ethanol concentration up to 60% (v/v) was tested. To achieve such a high concentration, the GO solution was first concentrated by centrifugation at 6000 rpm for 4 min followed by removal of the supernatant. About half of GO was lost during this process as estimated by UV-vis spectroscopy. In a final volume of 20 μL, each sample contained 1 μM of the 18-mer DNA, 90 μg/mL GO, 10 mM HEPES, pH 7.6, varying concentrations of ethanol, and 100 mM NaCl or no NaCl. Samples without GO were also prepared to calculate the adsorption efficiency by the equation (F_{noGO}-F_{GO})/F_{noGo}, where F_{noGO} and F_{GO} are the fluorescence intensity in the absence and presence of GO, respectively. The fluorescence was read by the real time PCR thermocycler.

Thermal Denaturation. Temperature induced desorption of DNA experiment was carried out in the real time PCR thermocycler using a sample volume of 20 μL. The DNA (500 nM) was adsorbed on the GO

surface (50 μg/mL) in the presence of 25 mM HEPES, pH 7.6 and 100 mM NaCl. For NaCldependent studies, different NaCl concentrations were tested. After incubating the sample at room temperature for 2 hr, the samples were transferred into a 96-well PCR plate and sealed with a plastic wrap for melting analysis. The temperature was increased every 1 °C with a holding time of 1 min before each reading.

Desorption by c-DNA. The DNA/GO complex was prepared by mixing 50 pmol of the 24-mer DNA and 20 μL of 200 μg/mL GO in 5 mM $MgCl_2$, 100 mM NaCl, and 25 mM HEPES, pH 7.6. This mixture was centrifuged to remove free DNA in the supernatant and then re-dispersed in 200 μL of the same buffer. The desorption experiment was carried out with the fluorescence plate reader. Each well contained 65 μL of the buffer with 15 μL of the DNA/GO complex solution. 20 μL of the c-DNA was then added to initiate the desorption reaction. Exchange of adsorbed DNA was studied using a similar method and the same 24-mer DNA without the fluorophore label was added.

AFM. The synthesized GO sheets were absorbed on a silicon chip, which was pretreated with piranha and (3-Aminopropyl)triethoxysilane. The characterization was carried out a Nanoscope IV AFM Instrument (Veeco).

Results and Discussion

Effect of Salt. In this study, we employed four FAM-labeled ss-DNAs with DNA lengths of 12, 18, 24, and 36-mer, respectively. None of the sequences can form highly stable secondary structures under experimental conditions and the difference in performance is therefore expected to be caused by their length. All the FAM labels are on the 5′-end of the DNAs. Upon exciting the 18-mer DNA at 485 nm, a strong FAM emission at 520 nm was observed (Figure 1D). Addition of GO brought the fluorescence to the baseline level. This is consistent with previous reports that GO can effectively quench the adsorbed FAM-DNA emission.[16,26] Therefore, the fluorescence quenching efficiency is directly proportional to the amount of DNA adsorbed and these two parameters can be used interchangeably. After adsorption, adding the complementary DNA (c-DNA), the same DNA, or increasing temperature may promote DNA

desorption, which is accompanied with a fluorescence enhancement. The scheme of this whole process is shown in Figure 1A.

The GO samples were prepared by the modified Hummers method and were imaged by AFM after deposition on a silicon wafer. As shown in Figure 1B and C, the height of the GO sheets is ~ 1.5 nm. This confirms that they are monolayer GO and in solution they exist primarily as exfoliated single sheets. This also occurs due to oxidation of the sheets leading to a net negative charge on them. The GO prepared by this method has ~15% crystalline graphene regions on the sheet with the remaining 85% being amorphous carbon like.[46] The size of the GO sheet ranges from several tens of nanometer to several micrometers.

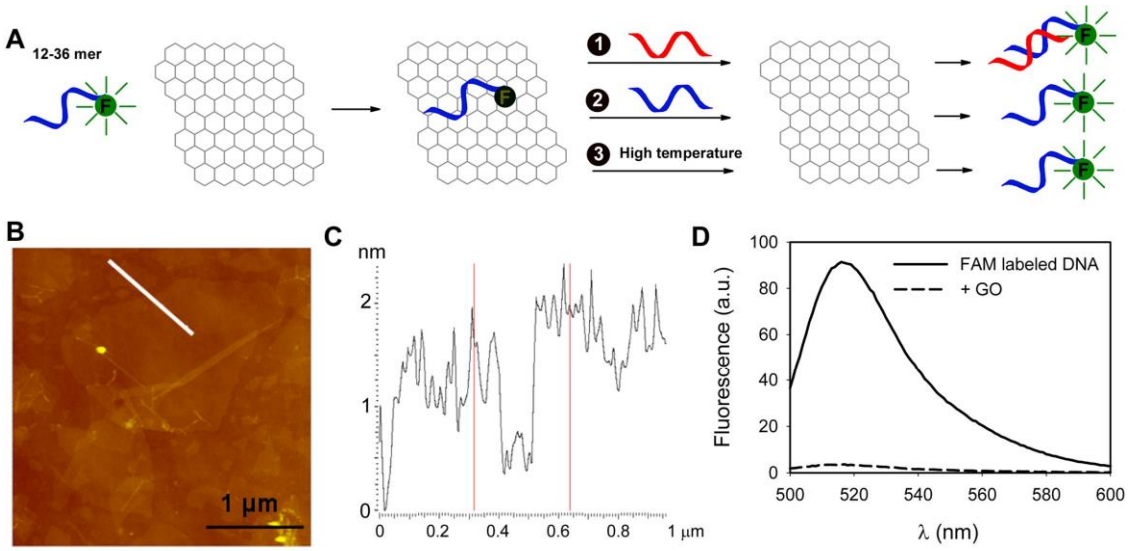

Figure 1. (A) Schematic presentation of FAM-labeled DNA adsorption and desorption on GO. Fluorescence is quenched upon adsorption. Desorption can be achieved by adding the c-DNA (reaction 1), DNA exchange with the same DNA (reaction 2), or increasing temperature (reaction 3). (B) An AFM image showing GO sheets deposited on a silicon wafer. (C) The height profile of the line in (B) shows the sheets to be ~ 1.5 nm in thickness. (D) Fluorescence spectra of 100 nM 18-mer DNA in 25 mM HEPES, 100 mM NaCl and 5 mM $MgCl_2$ in the presence and absence of 50 μg/mL of GO.

DNA is a polyanion and the surface of GO contains carboxylic acid groups that are deprotonated at neutral pH. Therefore DNA should be repelled by the negatively charged GO due to electrostatic repulsion. On the other hand, DNA bases contain aromatic and hydrophobic rings that can bind to GO through hydrophobic interactions and π-π stacking.[34-36] To facilitate these short-range interaction, however, electrolytes are needed to screen the long-range electrostatic repulsion and bring DNA close to the GO surface for binding.

As shown in Figure 2A, in absence of salt (i.e. just in pure water), the quenching efficiency was less than 30% for all the four DNA lengths, confirming that the binding was quite weak. Significant quenching was observed with even 10 mM NaCl. At higher NaCl concentrations, the quenching efficiencies were progressively better. For example, with 100 mM NaCl, the quenching was close to 100% for the three short DNAs. We noticed that the quenching efficiency was lower for the longer DNAs, suggesting weaker binding. This may result from the structure of GO which is reported as being composed of intact crystalline regions where hydrophobic interactions with DNA dominate and defective amorphous regions (oxidized) that contain the anionic functionalization which repel the DNA.[47] The size of both the domains is on the scale of 5-8 nm.[47] The 36-mer DNA has a radius of gyration of ~5 nm,[48] close to the domain size in GO and hence its adsorption is likely to be limited by the repulsive interaction with the amorphous region. Length dependent DNA binding to inorganic surfaces has also been observed for gold nanoparticles, where short DNAs were also more effective in binding and stabilizing colloidal gold.[49,50]

Next we tested the effect of divalent Mg^{2+} ions. With greater than 1 mM Mg^{2+}, the quenching efficiencies were close to 100% for all the sequences (Figure 2B). This is consistent with the concept that divalent metal ions are much more effective in screening charges and acting as a bridge to connect two negatively charged molecules in comparison to monovalent ones.[51] The same length-dependent quenching was also observed at lower Mg^{2+} concentrations. The DNA concentrations used in all the experiments were 1 μM. Therefore, the concentrations of phosphate linkages ranged from 11 to 35 μM.

At a Mg^{2+} concentration of 100 μM, the number of phosphate and Mg^{2+} became comparable. As shown in Figure 2B, 100 μM Mg^{2+} induced ~90% quenching for the 12-mer DNA. For the 36-mer DNA, the quenching was close to 50%. This confirms a very high affinity of binding between Mg^{2+} and the DNA phosphate to allow almost quantitative interaction (e.g. the K_d between Mg^{2+} and DNA was determined to be ~0.6 μM.[52]).

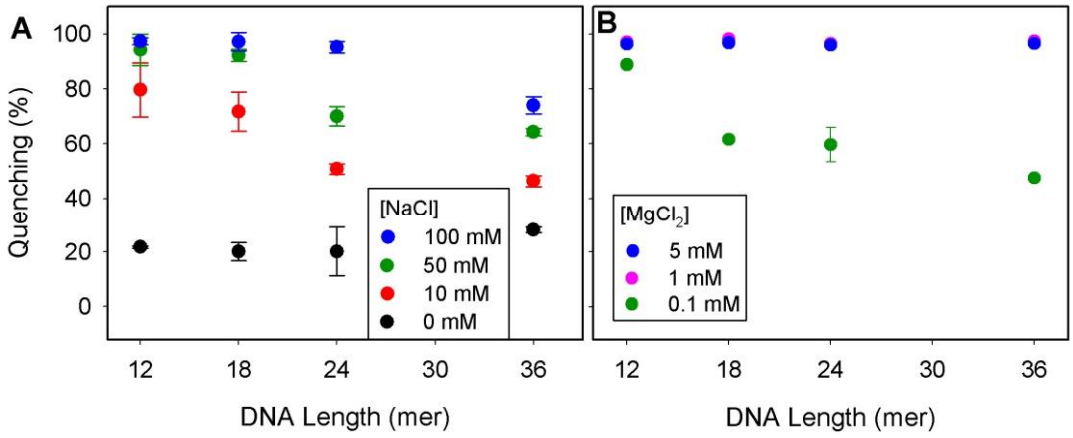

Figure 2. Quenching efficiency as a function of DNA length in the presence of varying concentrations of NaCl (A) or $MgCl_2$ (B). The quenching was mainly due to adsorption of DNA on the GO surface. The DNA concentrations for GO and DNA were 170 μg/mL and 1 μM, respectively.

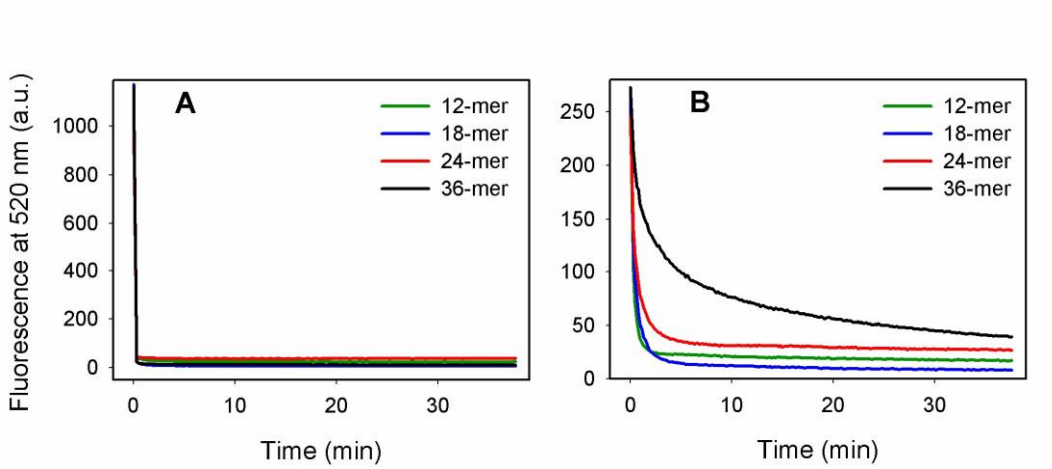

Figure 3. DNA length-dependent adsorption kinetics at high (A) and low (B) reactant concentrations. In (A), DNA concentration = 200 nM, GO = 40 μg/mL with 4 mM $MgCl_2$ and 80 mM NaCl. In (B), DNA concentration = 50 nM, GO = 5 μg/mL with 1 mM $MgCl_2$ and 20 mM NaCl.

Kinetics of Binding. In the above salt-dependent studies, the sample fluorescence was measured at ~5 min after mixing DNA with GO, and close to complete quenching was observed for many of the samples, suggesting fast binding kinetics. To quantitatively characterize binding, we next monitored the kinetics of DNA binding to the GO surface. With a high concentration of DNA (200 nM), GO (40 μg/mL), and salt (4 mM $MgCl_2$, 80 mM NaCl, and 20 mM HEPES, pH 7.6), the adsorption occurred instantaneously for all the DNAs. As shown in Figure 3A, the adsorption was completed in less than 20 sec. To test whether there is a difference among the different DNAs, the concentrations of the reactants were reduced to 50 nM DNA, 5 μg/mL GO, 1 mM $MgCl_2$, 20 mM NaCl, and 20 mM HEPES to decrease the rate of binding. As shown in Figure 3B, the longer DNAs showed slower adsorption kinetics, which is consistent with previous reports using different DNA sequences.[16]

Effect of pH. Since electrostatic interactions play a crucial role in determining the binding between DNA and GO, in addition to tuning ionic strength, changing solution pH is another useful means to control

surface charge. GO was proposed to contain several types of carboxylic acid groups that bear slightly different pK_a's.[53] A schematic presentation of GO surface functional groups is shown in Figure 4A. Since FAM is a pH-sensitive fluorophore and its quantum yield is close to zero at pH's lower than 4, a direct comparison of the quenching efficiency is difficult at low pH. Therefore, the pH effect was studied by an indirect method. Five buffers were prepared ranging from pH 4 to 8 and the 36-mer DNA was mixed with GO in the buffers containing also 10 mM NaCl. After incubation at room temperature for 1 hr, the samples were centrifuged at 15000 rpm for 20 min and all the GO was precipitated. The supernatant solution containing only the free DNA was collected and diluted 10 times in a pH 8.3 buffer for fluorescence measurement. As can be observed in Figure 4B, the binding was more effective at lower pH. For example, by lowering the pH from 8 to 5, the binding increased from 30% to 100%. Therefore, the binding strength can be conveniently controlled by tuning the solution pH.

The GO surface is terminated by several different carboxylic acid groups as shown in Figure 4A, and the pK_a values of these groups should be close to that of benzoic acid (pK_a=4.2) or acetic acid (pK_a=4.7). At neutral pH, these groups are depronated to give a highly negatively charged surface. At close to the pK_a's, the surface charge is neutralized to reduce repulsion. While for DNA, the phosphate group has a pK_a close to zero. Therefore, the DNA backbone negative charge is always maintained in the pH range tested. Only the N3 position of cytosine can be protonated at pH 4 (pK_a=4.2), which may also contribute to a reduced repulsion. In addition to the reduction of electrostatic repulsion, protonation of carboxylic acid groups on GO should also make the hydrophobic interaction stronger as the surface becomes less polar.

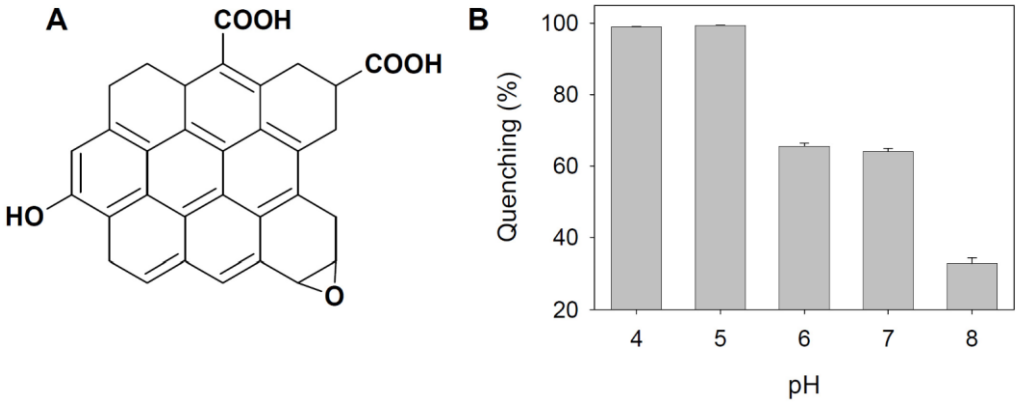

Figure 4. (A) Schematic presentation of some of the surface functional groups on a small fraction of GO surface. Two representative types of proposed carboxylic acid groups on the surface are shown. (B) Quenching efficiency as a function of pH with the 36-mer DNA. Each sample (40 μL) contained a final buffer concentration of 50 mM, 10 mM NaCl, 170 μg/mL of GO and 1 μM of the 36-mer DNA.

Effect of Organic Solvents. Using organic solvents such as ethanol may provide insights on both electrostatic and hydrophobic interactions. Therefore, the binding of the 18-mer DNA as a function of ethanol concentration was studied. As shown in Figure 5 (open squares), when the no NaCl was present, the quenching or binding efficiency decreased from the initial value of 40% in water (with just 10 mM HEPES, pH 7.6 and no additional NaCl) to close to 0% with 60% ethanol. The lower dielectric constant of ethanol compared to water amplified the electrostatic repulsion between DNA and GO, resulting in reduced absorption. At the same time, ethanol is less polar than water and hence a better solvent for hydrophobic molecules, which should decrease the hydrophobic interaction between DNA and GO in ethanol. Taking together, the binding between DNA and GO at low salt was weakened by ethanol as shown in Figure 5.

Interestingly, in presence of 100 mM NaCl, higher ethanol concentration increased the quenching efficiency (Figure 5, solid dots), suggesting a stronger DNA adsorption. We attribute this observation to

a reduced electrostatic repulsion. With a higher ethanol concentration the dielectric constant of solution is decreased, making Na^+ more effective in screening the charges on DNA and GO to reduce repulsion. Further we observed that with 100 mM NaCl, GO lost its colloidal stability even in the presence of 15% ethanol; while in the absence of NaCl the GO solution was stable with up to 60% ethanol. In water (no ethanol) our GO is stable at 100 mM NaCl. These observations confirm that a combination of NaCl and ethanol screens the surface charges of GO very effectively.

Based on these results we concur that when the hydrophobic interactions are weak (e.g. with 60% ethanol), the electrostatic interaction dominate the DNA adsorption behavior. In such conditions almost no absorption is observed at low salt concentration. Conversely, with stronger hydrophobic interaction (e.g. with 0% ethanol) significant DNA absorption (~ 40%) can be achieved even when the electrostatic repulsion was strong (e.g. in absence of NaCl).

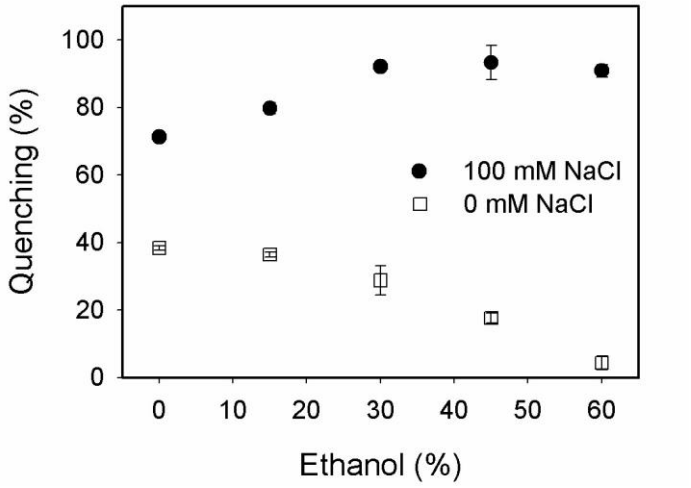

Figure 5. Quenching efficiency of the 18-mer DNA as a function of ethanol concentration (v/v) in low or high salt buffers. All the samples contained 10 mM HEPES, pH 7.6. The final DNA concentration was 1 μM and GO concentration was ~90 μg/mL.

Desorption by c-DNA and DNA Exchange. It is known that adsorbed DNA can be desorbed by the addition of the c-DNA.[15] This is the basis of using GO for DNA detection and it provides a further piece of evidence that hydrophobic interactions are extremely important for the adsorption of DNA on GO. Upon forming ds-DNA, the DNA bases are hidden inside the helical structure and no long available for surface binding; only the negatively charged phosphate groups are exposed. Therefore, desorption is likely to occur due to the disruption of hydrophobic interactions.

To study the c-DNA induced desorption as shown in Figure 1A (reaction 1), GO samples with saturating amount of the 24-mer DNA on the surface was prepared and the free DNA was removed by centrifugation. The GO/DNA complex was then re-dispersed in buffer. Upon addition of the c-DNA, a fast fluorescence increase was observed as shown in Figure 6A; higher concentration of the c-DNA gave faster desorption kinetics. In the absence of the c-DNA, the fluorescence was still quenched. After 30 min, ~70% of DNA was desorbed in the presence of 800 nM c-DNA. If sufficient time was allowed (e.g. after overnight incubation), complete desorption was achieved since the final fluorescence intensity reached a value close to the ds-DNA sample without GO (difference within 5%).

Desorption by forming ds-DNA suggests that the DNA binding is reversible. To further understand the desorption property; the exchange of adsorbed DNA with free DNA in solution was also studied (Figure 1A, reaction 2). With the same 24-mer FAM-DNA covered GO, as prepared above, varying concentration of the same DNA sequence but without the fluorophore label was added. As shown in Figure 6B, DNA concentration dependent desorption was also observed and a higher added DNA concentration produced a faster exchange rate. For the same DNA concentration, the desorption kinetics (with the c-DNA) were faster than the exchange kinetics.

Since in the absence of the non-labeled DNA no desorption was detected, the exchange process is likely to take place through first adsorption of the non-labeled DNA followed by desorption of the labeled one due to electrostatic repulsion between DNA. This observation may help optimize GO-based sensors for DNA detection. In the above experiments, the GO surface was saturated with the FAMlabeled DNA. While a high loading of fluorophore-labeled DNA probes may allow a higher sensitivity, the exchange of

adsorbed DNA by non-target DNA may generate false positive signals. Since there is a limited DNA adsorption capacity on GO (see Supporting Information), to effectively detect target DNA with high specificity, free surface binding sites should exist to accommodate additional DNA in solution so that they can react on the GO surface. Once a ds-DNA is formed, it can then be desorbed to give a fluorescence signal. If the surface is saturated by the fluorescent probe DNA, even non-target DNA can compete with the probe DNA to result in a false positive signal (see Supporting Information).

Exchange of adsorbed biomacromolecules has been studied in many systems, mostly with proteins. For example, with a carbon surface, the adsorption of albumin and fibrinogen was very strong and little exchange occurred. But for a silica surface, the same proteins were reversibly adsorbed.[54] DNA adsorption appears to be more reversible. For example, DNA adsorption on silica,[55] mica,[56] ziconia,[57] polymer,[58,59] and carbon nanotubes[60] have all been reported. The exchange of adsorbed DNA by the same DNA, however, has not been found in the literature.

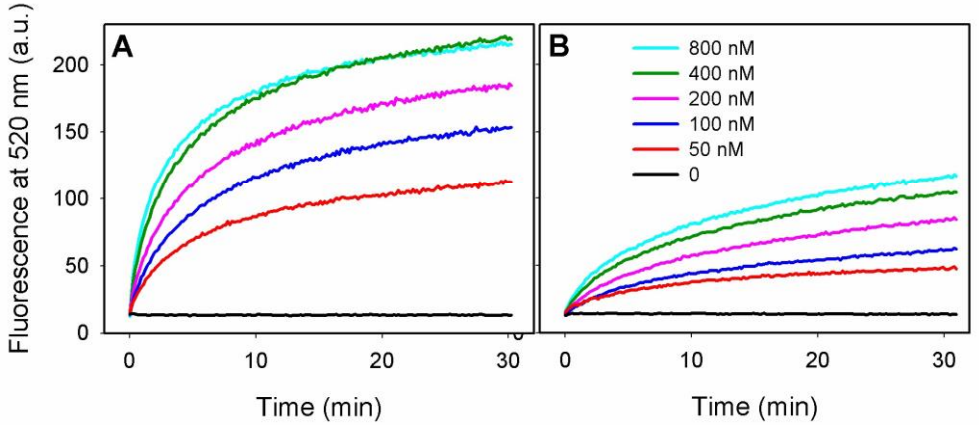

Figure 6. Kinetics of DNA desorption from GO surface induced by adding the c-DNA (A) and through exchange by adding the same DNA but without the FAM label (B). The 24-mer DNA was used for the experiment. The figure legend in (B) is shared by the two figures.

Thermal Desorption. In addition to DNA induced desorption described above, increase of temperature is also expected to facilitate desorption.[31,61] Therefore, the thermal dissociation of adsorbed DNA was also studied. In a typical experiment, a sample volume of 20 μL was prepared containing 500 nM DNA, 50 μg/mL GO, 100 mM NaCl and 25 mM HEPES, pH 7.6. The same samples without GO were also prepared for comparison. Thermal dissociation should lead to an increased fluorescence as shown in Figure 1A (reaction 3).

The temperature-dependent fluorescence changes of the four DNAs are shown in Figure 7A-D (red curves for samples with GO and black curves for samples without GO). For all the GO containing samples, the fluorescence values remained much lower compared to those of free DNAs even at 95 °C. This suggests that it is quite ineffective to desorb DNA by increasing temperature. For practical applications, however, this temperature insensitivity may be useful to give a temperature-independent background.

If the fluorescence of the GO containing samples was compared, increased fluorescence can be observed for the 18, 24, and 36-mer samples in the temperature region from 25 to 65 °C (Figure 7F). At higher temperature, the fluorescence decreased due to reduced quantum yield of the fluorophore. The relative amount of desorption was the largest for the 36-mer DNA and the smallest for the 12-mer DNA.
This is also consistent with the previous studies that the shorter DNAs were more effectively adsorbed. No obvious melting transitions were observed for all tested samples and desorption occurred over a wide temperature range, which is consistent with previous literature report.[31] As shown in Figure 7G, the 18, 24, and 36-mer DNA all showed the largest transition around 60 □C, suggesting that the relative rate of desorption does not depend on the DNA length.

We also tested the adsorption of the fluorophore (fluorescein) on the GO surface and interestingly, a significant amount of quenching was also achieved (Figure 7E), suggesting this negatively charged fluorophore can be effectively adsorbed by GO. Increasing temperature of this sample resulted in dissociation of the fluorophore from the surface (Figure 7F, red curve). The amount of desorption was

much larger compared to those observed with the DNA samples, suggesting that the DNA binding to the surface was much stronger than the single fluorophores.

The effect of salt concentration (NaCl) on the thermal dissociation of the 24-mer DNA is presented in Figure 7H. The amount of desorbed DNA decreased with increasing salt. At concentrations higher than 200 mM NaCl, very little desorption was observed. This is consistent with the observations that higher salt leads to a stronger interaction of the DNA with GO, hence reducing thermal desorption of the absorbed DNA.

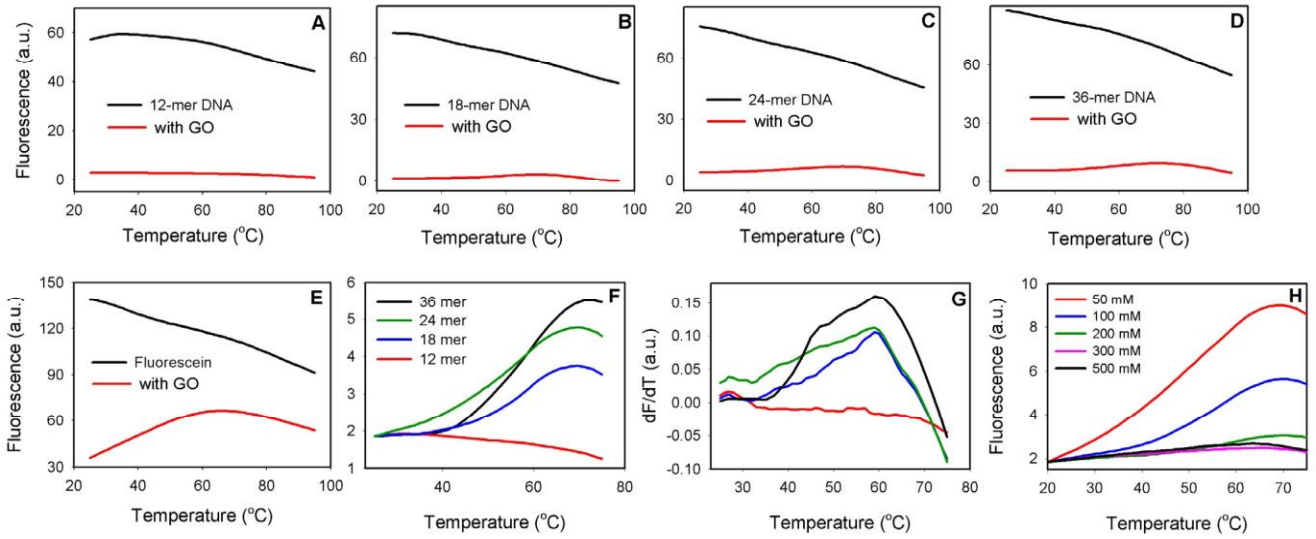

Figure 7. Thermal desorption profiles of adsorbed DNA. (A-D) Temperature dependent fluorescence change of free DNA and DNA associated with GO. (E) Desorption of fluorescein. (F) Comparison of DNA length dependent thermal desorption. The curves are normalized to have the same starting fluorescence value at 25 °C. (G) The first derivatives of the melting curves in (F). (H) NaCl concentration dependent desorption of the 24-mer DNA.

Conclusions. In summary we have systematically studied the adsorption and desorption of fluorescently labeled oligonucleotides on GO surface. The binding between DNA and GO is strongly affected by both electrostatic repulsion and hydrophobic interactions. Cations, pH, and organic solvent can all be used to

modulate DNA binding. Shorter DNA binds to the surface with faster kinetics and higher adsorption efficiency. Desorption can occur by adding the c-DNA to form ds-DNA, adding the same DNA to exchange, and increasing temperature. The temperature induced desorption, however, was quite ineffective, suggesting a high binding affinity. Overall, the DNA binding to GO is very stable and reversible. These basic understandings of the surface interaction between DNA and GO are valuable for design and optimization of sensors and devices based on these molecules and materials.

ACKNOWLEDGMENTS. Funding for this work is from the University of Waterloo and the Discovery Grant from the Natural Sciences and Engineering Research Council of Canada (NSERC).

REFERENCES

(1) Novoselov, K. S.; Geim, A. K.; Morozov, S. V.; Jiang, D.; Zhang, Y.; Dubonos, S. V.; Grigorieva, I. V.; Firsov, A. A. *Science* **2004**, *306*, 666-669.

(2) Geim, A. K.; Novoselov, K. S. *Nat. Mater.* **2007**, *6*, 183-191.

(3) Allen, M. J.; Tung, V. C.; Kaner, R. B. *Chem. Rev.* **2009**, *110*, 132-145.

(4) Rao, C. N. R.; Sood, A. K.; Subrahmanyam, K. S.; Govindaraj, A. *Angew. Chem. Int. Ed.* **2009**, *48*, 7752-7777.

(5) Kim, K. S.; Zhao, Y.; Jang, H.; Lee, S. Y.; Kim, J. M.; Kim, K. S.; Ahn, J.-H.; Kim, P.; Choi, J.Y.; Hong, B. H. *Nature* **2009**, *457*, 706-710.

(6) Wu, J.; Agrawal, M.; Becerril, H. c. A.; Bao, Z.; Liu, Z.; Chen, Y.; Peumans, P. *Acs Nano* **2009**, *4*, 43-48.

(7) Shao, Y. Y.; Wang, J.; Wu, H.; Liu, J.; Aksay, I. A.; Lin, Y. H. *Electroanalysis* **2010**, *22*, 1027-1036.

(8) Schedin, F.; Geim, A. K.; Morozov, S. V.; Hill, E. W.; Blake, P.; Katsnelson, M. I.; Novoselov, K. S. *Nat. Mater.* **2007**, *6*, 652-655.

(9) Cheng, Z. G.; Li, Q.; Li, Z. J.; Zhou, Q. Y.; Fang, Y. *Nano Lett.* **2010**, *10*, 1864-1868.

(10) Castro Neto, A. H.; Guinea, F.; Peres, N. M. R.; Novoselov, K. S.; Geim, A. K. *Rev. Mod. Phys.* **2009**, *81*, 109-162.

(11) Sharma, R.; Baik, J. H.; Perera, C. J.; Strano, M. S. *Nano Lett.* **2010**, *10*, 398-405.

(12) Mohanty, N.; Berry, V. *Nano Lett.* **2008**, *8*, 4469-4476.

(13) Ohno, Y.; Maehashi, K.; Yamashiro, Y.; Matsumoto, K. *Nano Lett.* **2009**, *9*, 3318-3322.

(14) Dong, X.; Shi, Y.; Huang, W.; Chen, P.; Li, L. J. *Adv. Mater.* **2010**, *22*, 1649-1653.

(15) Lu, C. H.; Yang, H. H.; Zhu, C. L.; Chen, X.; Chen, G. N. *Angew. Chem. Int. Ed.* **2009**, *48*, 4785-4787.

(16) He, S. J.; Song, B.; Li, D.; Zhu, C. F.; Qi, W. P.; Wen, Y. Q.; Wang, L. H.; Song, S. P.; Fang, H. P.; Fan, C. H. *Adv. Funct. Mater.* **2010**, *20*, 453-459.

(17) Dong, H. F.; Gao, W. C.; Yan, F.; Ji, H. X.; Ju, H. X. *Anal. Chem.* **2010**, *82*, 5511-5517.

(18) Li, F.; Huang, Y.; Yang, Q.; Zhong, Z. T.; Li, D.; Wang, L. H.; Song, S. P.; Fan, C. H. *Nanoscale* **2010**, *2*, 1021-1026.

(19) Liu, F.; Choi, J. Y.; Seo, T. S. *Biosens. Bioelectron.* **2010**, *25*, 2361-2365.

(20) Lu, C. H.; Li, J.; Liu, J. J.; Yang, H. H.; Chen, X.; Chen, G. N. *Chem. Eur. J.* **2010**, *16*, 4889-4894.

(21) Chang, H. X.; Tang, L. H.; Wang, Y.; Jiang, J. H.; Li, J. H. *Anal. Chem.* **2010**, *82*, 2341-2346.

(22) Jang, H.; Kim, Y. K.; Kwon, H. M.; Yeo, W. S.; Kim, D. E.; Min, D. H. *Angew. Chem. Int. Ed.* **2010**, *49*, 5703-5707.

(23) Jung, J. H.; Cheon, D. S.; Liu, F.; Lee, K. B.; Seo, T. S. *Angew. Chem. Int. Ed.* **2010**, *49*, 5708-5711.

(24) Wen, Y. Q.; Xing, F. F.; He, S. J.; Song, S. P.; Wang, L. H.; Long, Y. T.; Li, D.; Fan, C. H. *Chem. Comm.* **2010**, *46*, 2596-2598.

(25) Song, Y. J.; Qu, K. G.; Zhao, C.; Ren, J. S.; Qu, X. G. *Adv. Mater.* **2010**, *22*, 2206-2210.

(26) Wang, Y.; Li, Z. H.; Hu, D. H.; Lin, C. T.; Li, J. H.; Lin, Y. H. *J. Am. Chem. Soc.* **2010**, *132*,

9274-9276.

(27) Lu, C.-H.; Li, J.; Lin, M.-H.; Wang, Y.-W.; Yang, H.-H.; Chen, X.; Chen, G.-N. *Angew. Chem., Int. Ed.* **2010**, *49*, 8454-8457.

(28) Lu, C. H.; Zhu, C. L.; Li, J.; Liu, J. J.; Chen, X.; Yang, H. H. *Chem. Comm.* **2010**, *46*, 3116-3118.

(29) Liu, Z.; Robinson, J. T.; Sun, X. M.; Dai, H. J. *J. Am. Chem. Soc.* **2008**, *130*, 10876-10877.

(30) Yang, X.; Zhang, X.; Ma, Y.; Huang, Y.; Wang, Y.; Chen, Y. *J. Mater. Chem.* **2009**, *19*, 2710-2714.

(31) Tang, Z. W.; Wu, H.; Cort, J. R.; Buchko, G. W.; Zhang, Y. Y.; Shao, Y. Y.; Aksay, I. A.; Liu, J.; Lin, Y. H. *Small* **2010**, *6*, 1205-1209.

(32) Manohar, S.; Mantz, A. R.; Bancroft, K. E.; Hui, C.-Y.; Jagota, A.; Vezenov, D. V. *Nano Lett.* **2008**, *8*, 4365-4372.

(33) Varghese, N.; Mogera, U.; Govindaraj, A.; Das, A.; Maiti, P. K.; Sood, A. K.; Rao, C. N. R. *ChemPhysChem* **2009**, *10*, 206-210.

(34) Ortmann, F.; Schmidt, W. G.; Bechstedt, F. *Phys. Rev. Lett.* **2005**, *95*, 186101.

(35) Gowtham, S.; Scheicher, R. H.; Ahuja, R.; Pandey, R.; Karna, S. P. *Phys. Rev. B* **2007**, *76*, 033401.

(36) Antony, J.; Grimme, S. *Phys. Chem. Chem. Phys.* **2008**, *10*, 2722-2729.

(37) Zheng, M.; Jagota, A.; Semke, E. D.; Diner, B. A.; McLean, R. S.; Lustig, S. R.; Richardson, R. E.; Tassi, N. G. *Nat. Mater.* **2003**, *2*, 338-342.

(38) Manohar, S.; Mantz, A. R.; Bancroft, K. E.; Hui, C. Y.; Jagota, A.; Vezenov, D. V. *Nano Lett.* **2008**, *8*, 4365-4372.

(39) Zhao, X.; Johnson, J. K. *J. Am. Chem. Soc.* **2007**, *129*, 10438-10445.

(40) Jeng, E. S.; Barone, P. W.; Nelson, J. D.; Strano, M. S. *Small* **2007**, *3*, 1602-1609.

(41) Heller, D. A.; Jeng, E. S.; Yeung, T.-K.; Martinez, B. M.; Moll, A. E.; Gastala, J. B.; Strano, M.

S. *Science* **2006**, *311*, 508-511.

(42) Yang, R. H.; Jin, J. Y.; Chen, Y.; Shao, N.; Kang, H. Z.; Xiao, Z.; Tang, Z. W.; Wu, Y. R.; Zhu, Z.; Tan, W. H. *J. Am. Chem. Soc.* **2008**, *130*, 8351-8358.

(43) Yamamoto, Y.; Fujigaya, T.; Niidome, Y.; Nakashima, N. *Nanoscale* **2010**, *2*, 1767-1772.

(44) Hummers, W. S.; Offeman, R. E. *J. Am. Chem. Soc.* **1958**, *80*, 1339-1339.

(45) Marcano, D. C.; Kosynkin, D. V.; Berlin, J. M.; Sinitskii, A.; Sun, Z.; Slesarev, A.; Alemany, L. B.; Lu, W.; Tour, J. M. *Acs Nano* **2010**, *4*, 4806-4814.

(46) Mkhoyan, K. A.; Contryman, A. W.; Silcox, J.; Stewart, D. A.; Eda, G.; Mattevi, C.; Miller, S.; Chhowalla, M. *Nano Lett.* **2009**, *9*, 1058-1063.

(47) Gomez-Navarro, C.; Meyer, J. C.; Sundaram, R. S.; Chuvilin, A.; Kurasch, S.; Burghard, M.; Kern, K.; Kaiser, U. *Nano Lett.* **2010**, *10*, 1144-1148.

(48) Tinland, B.; Pluen, A.; Sturm, J.; Weill, G. *Macromolecules* **1997**, *30*, 5763-5765.

(49) Li, H.; Rothberg, L. J. *Anal. Chem.* **2004**, *76*, 5414-5417.

(50) Li, H.; Rothberg, L. J. *J. Am. Chem. Soc.* **2004**, *126*, 10958-10961.

(51) Liu, S.; Ghosh, K.; Muthukumar, M. *Journal of Chemical Physics* **2003**, *119*, 1813-1823.

(52) Rowatt, E.; Williams, R. J. P. *J. Inorg. Biochem.* **1992**, *46*, 87-97.

(53) Langley, L. A.; Villanueva, D. E.; Fairbrother, D. H. *Chem. Mater.* **2006**, *18*, 169-178.

(54) Feng, L.; Andrade, J. D. *Biomaterials* **1994**, *15*, 323-333.

(55) Kang, S. H.; Shortreed, M. R.; Yeung, E. S. *Anal. Chem.* **2001**, *73*, 1091-1099.

(56) Thomson, N. H.; Kasas, S.; Smith, B.; Hansma, H. G.; Hansma, P. K. *Langmuir* **1996**, *12*, 5905-5908.

(57) Liu, S. Q.; Xu, J. J.; Chen, H. Y. *Colloid. Surface. B.* **2004**, *36*, 155-159.

(58) Paril, C.; Horner, D.; Ganja, R.; Jungbauer, A. *J. Biotechnol.* **2009**, *141*, 47-57.

(59) Ganachaud, F.; Elaissari, A.; Pichot, C. *Langmuir* **1997**, *13*, 7021-7029.

(60) Carot, M. L.; Torresi, R. M.; Garcia, C. D.; Esplandiu, M. J.; Giacomelli, C. E. *J. Phys. Chem. C*

2010, *114*, 4459-4465.

(61) Herdt, A. R.; Drawz, S. M.; Kang, Y. J.; Taton, T. A. *Colloid. Surface. B.* **2006**, *51*, 130-139.